Impacts of meltwater discharge from marine-terminating glaciers on the protist community in Inglefield Bredning, northwestern Greenland

Running page head: Meltwater impacts on a protist community

Kohei Matsuno[1,2*], Naoya Kanna[2], Shin Sugiyama[2,3], Atsushi Yamaguchi[1,2],·Eun Jin Yang[4]

1: Graduate School of Fisheries Sciences, Hokkaido University, 3−1−1 Minato-cho, Hakodate, Hokkaido, 041-8611, Japan

2: Arctic Research Centre, Hokkaido University, Kita-21 Nishi-11 Kita-ku, Sapporo, Hokkaido, 001-0021, Japan

3: Institute of Low Temperature Science, Hokkaido University, Kita-19 Nishi-8 Kita-ku, Sapporo, Hokkaido, 060-0819, Japan

4: Division of Polar Ocean Science, Korea Polar Research Institute, 26 Songdomirae-ro, Yeonsu-gu, Incheon, 21990, Republic of Korea

* Corresponding author

E-mail, k.matsuno@fish.hokudai.ac.jp

Abstract

To evaluate the effects of meltwater discharge from marine-terminating glaciers on a fjord protist community in northwestern Greenland during summer, we investigated the distribution, abundance and biomass of the protist community and their relationships with hydrographic parameters. In the standing stock of protists, dinoflagellates (46.4%) and oligotrich ciliates (39.5%) were dominant throughout the study region. According to the vertical distribution, oligotrich ciliates were abundant in the surface layer, mainly due to suitable food conditions (abundance of diatom and nanoflagellates). Near glaciers, relatively high chl *a* concentrations were found in the subsurface layers associated with the low-temperature, high-turbidity and slightly high nutrient levels, indicating that the nutrient inputs from the upwelling glacial meltwater plume increased primary production. Large-sized *Protoperidium* spp. were found only at stations near glaciers where nutrients were abundant, and heterotrophic dinoflagellates showed strong relationships with nanoflagellates. These findings suggest that the upwelling associated with subglacial meltwater discharge can stimulate nanoflagellate production, resulting in increases in ciliate and heterotrophic dinoflagellate production.

Keywords: Protist community, Meltwater discharge, Marine-terminating glacier, Ciliates, Dinoflagellates

1. INTRODUCTION

Recently, tidewater glaciers in Greenland have been thinning and retreating under the influence of atmospheric and oceanic warming (e.g., Howat & Eddy 2011, Cowton et al. 2018). These glaciers flow directly into the ocean, forming important ice-ocean boundaries in glacial fjords. Near the glacier front in a fjord, subglacial discharge upwells cold and high-nutrient deep-water into euphotic zone (Bendtsen et al. 2015, Meire et al. 2017; Kanna et al., 2018), inducing high primary production throughout summer in the fjord (Arendt et al. 2013, Juul-Pedersen et al. 2015, Meire et al. 2017, Kanna et al. 2018). By contrast, this upwelling does not occur in fjords with land-terminating glaciers, which are characterized by lower productivity (Meire et al. 2017, Middelbo et al. 2018). The amount and type of inflow (surface or subsurface) of freshwater into the fjord may influence fjord water circulation, nutrient availability and subsequent productivity (Mortensen et al. 2011, Lydersen et al. 2014).

Ciliates and heterotrophic dinoflagellates (HDF), which have frequently been observed to ingest bacteria, autotrophic nanoflagellates and diatoms (Gast 1985, Paranjape 1987, Sherr et al. 2003; Calbet et al. 2011), are abundant in Arctic marine systems during summer (Sherr et al. 1997, Rysgaard et al. 1999, Seuthe et al. 2011). Additionally, heterotrophic nanoflagellates (HNF) are the essential link from bacteria to

the ciliates and the HDFs. These heterotrophic organisms are preyed upon by mesozooplankton (Levinsen et al. 2000, Levinsen & Nielsen 2002); thus, they play important roles in the microbial loop (Pomeroy 1974). In Arctic marine waters, the species compositions of the protist communities are typically dominated by athecate dinoflagellates and oligotrich ciliates, whereas thecate dinoflagellates and tintinnids show low abundances (Levinsen & Nielsen 2002; Krawczyk et al. 2015). For heterotrophic organisms, their biomasses are influenced by phytoplankton blooms in the Arctic Ocean (Taniguchi 1984, Sherr et al. 1997, Olson & Strom 2002). In the Disko Bay, oligotrich ciliates and HDFs have been found to be the dominant members of the protist community during summer (Levinsen et al. 2000, Levinsen & Nielsen 2002). Their biomasses peak during this time due to decreases in the top-down effect that are driven by the absence of large copepods from the euphotic zone in early spring and late summer (Levinsen & Nielsen 2002).

Around Greenland, the features of the protist community have been studied in Disko Bay (Nielsen & Hansen 1995, Levinsen et al. 1999, Levinsen et al. 2000), in Young Sound (Rysgaard et al. 1999, Rysgaard & Nielsen 2006, Krawczyk et al. 2015) and in Godthåbsfjord (Arendt et al. 2010, Calbet et al. 2011). However, beyond these regions, there are few studies and no information is available regarding the protist

communities in northwestern Greenland. In addition, the impacts of meltwater discharges from glaciers on bacterial production (Paulsen et al. 2017), primary production (Arendt et al. 2013, Juul-Pedersen et al. 2015, Meire et al. 2017) and zooplankton (Arendt et al. 2016) have been reported in Greenland, and the distributions of protist communities in Greenlandic fjords have been studied (e.g., Nielsen & Hansen 1995, Rysgaard et al. 1999). However, the impacts of meltwater discharge on protists are not fully understood.

In this study, we revealed the spatial distributions of protists (diatoms, dinoflagellates, ciliates and nanoflagellates) in Inglefield Bredning, a ~100-km long and ~20-km wide glacial fjord in northwestern Greenland. Recent studies in this region have revealed the importance of meltwater discharge from a marine-terminating glacier for biogeochemical processes in fjords (Kanna et al. 2018, Naito et al. 2019). Inglefield Bredning is fed by retreating marine-terminating glaciers (Sakakibara and Sugiyama 2018) and glacial changes are possibly affecting marine ecosystems. Based on sampling and hydrographic observations, we evaluated the impacts of meltwater discharges from marine-terminating glaciers on the biomasses of the protist community during summer.

2. MATERIALS & METHODS

2.1. Field sampling

Boat-based observations were performed during daytime over 13-17 August 2018 in the northeastern section of Inglefield Bredning (Fig. 1). The study area includes regions that are within several kilometers from Sharp and Hart Glaciers, as well as the region ~10 km from Melville Glacier. These glaciers discharge meltwater and icebergs into the fjord through calving fronts that are several kilometers wide (Sakakibara and Sugiyama 2018). Temperature, salinity, fluorescence, turbidity (Formazin Turbidity Units: FTU) and dissolved oxygen (DO) were measured with a current, temperature and depth (CTD) profiler (ASTD 102, JFE Advantech, Japan) at six stations. At these stations, water samples (500 mL) were collected by Niskin-X bottles (General Oceanics, Inc.) from 0, 10 m, 20 m, 30 m, 40 m, 50 m, 70 m, and 100 m depth at all six stations except for St. 4, where samples were collected from 0 m - 40 m (Fig. 1). The samples were fixed with 1% glutaraldehyde. For the nutrient and chl *a* measurements, seawater samples were collected from five to eight depths (e.g., 0 m, 10 m, 20 m, 30 m, 40 m, 50 m, 70 m, and 100 m, depending on bottom depth). For the chl *a* measurements, 100 mL of seawater from each sample was filtered on a GF/F filter. The filtered sample was immersed in N,N-dimethylformamide (Wako Pure Chemical Industries, Ltd.) under dark conditions for 24 h. The samples for nutrient and chl *a* (extracted in

N,N-dimethylformamide) analyses were immediately placed in a freezer (−20°C), transported to Japan without melting, and then stored in a cold laboratory (−20°C) until analysis. The nutrients (nitrate, nitrite, phosphate and silicic acid) in seawater were analyzed using an autoanalyzer (QuAAtro, BL TEC, Inc.) after sample filtration using syringe GF/F filters. The measurements of all nutrients were quality controlled by using reference seawater materials (KANSO Technos Co., Ltd.). Chl *a* was measured with a fluorometer (Turner Designs, Inc., 10-AU) using the nonacidification method of Welshmeyer (1994).

2.2. Microscopic analysis

In the laboratory, the 500-mL water samples were stored on a stone table for more than 1 day to allow the microprotist cells to settle to the bottom of each bottle. Then, the samples were concentrated to 20 mL using a siphon. Subsamples (0.25-1 mL) were mounted on glass microscope slides with lines and the diatoms, dinoflagellates and ciliates were counted and identified to the species/genus levels under an inverted microscope with 40–400× magnification. Nanoflagellates, i.e., flagellates with cell sizes of 5-10 μm, were also counted, but their cell densities might have been underestimated due to their small size. All of the nanoflagellates were classified as

autotrophic/mixotrophic/heterotrophic because we did not check the cells having chloroplasts or by not using microscopic epifluorescence. We enumerated 8–2,272 protist cells (including nanoflagellates) per sample. As we concentrated each sample from a volume of 500 mL to a volume of 20 mL, the limit of detection was 160 cells L^{-1} for each 0.25-mL subsample and was 40 cells L^{-1} for each 1-mL subsample.

Species identifications were made to the lowest possible level (e.g., species or genus) (Table 1). For species identification, we referred to Hasle and Syvertsen (1997) for diatoms, Fukuyo et al. (1997) and Evagelopoulos (2002) for dinoflagellates, and Maeda (1997) and Taniguchi (1997) for ciliates. Silicoflagellates and cysts of each taxon were omitted from the following analyses due to their low densities. Our preservative (glutaraldehyde) is an adequate fixative for diatoms and dinoflagellates but not for ciliates. Because ciliates are better preserved with acidic Lugol's solution (Stoecker et al. 1994) than with glutaraldehyde, our preservative may have led to biased estimates of community structure and biomass (through the loss of unloricated ciliates).

Using the cell sizes (length and width) measured during the counting process, the protist biovolumes were calculated following the method reported by Sun and Liu (2003). Then, the carbon biomasses were estimated using the carbon-volume relationship proposed by Menden-Deuer and Lassard (2000). Finally, the biomasses (µg

C L^{-1}) were calculated from the carbon biomass per cell and from the abundances (cells L^{-1}).

2.3. Data analysis

To evaluate the environmental factors controlling the changes in the protist community, we applied Structural Equation Modeling (SEM) analysis (Stomp et al. 2011). For the SEM analysis, the environmental parameters (temperature, salinity, turbidity, silicate and chl *a*) and the biomass of each protist taxon were normalized (average = 0, standard deviation = 1), and regressions among all parameters were calculated. For the path analysis, we set the parameters for three categories (1: temperature, salinity, turbidity, and silicate; 2: chl *a*, diatoms, and nanoflagellates; 3: dinoflagellates, oligotrich ciliates, and tintinnids). Subsequently, parameters with insignificant relationships ($p > 0.05$) were removed from the final model (cf. Matsuno et al. 2016). The SEM analysis was performed using add-in software for MS-Excel (http://www.ohmsha.co.jp/data/link/978-4-274-06925-3/).

3. RESULTS

3.1. Environmental conditions

The surface water temperatures ranged from 0.67 to 4.3ºC (Fig. 2). The temperatures between 0 and 20 m depth were lower at St. 4 and 5 than at the other stations. The salinities in the surface layer ranged from 27.5 to 30.2 and, similar to temperature, were lower at stations near the glacier (i.e., St. 4 and St. 5) than at those in the downfjord region (Fig. 2). The turbidity levels showed marked differences among the stations. Near glaciers, high turbidities were observed below 50 m at St. 5 and St. 6 and at approximately 10 m at St. 4 and St. 5. The fluorescence and chl *a* levels showed similar patterns. High chl *a* concentrations were observed near 10 m at the near-glacier stations and relatively high values were observed near 75 m at St. 2, St. 3 and St. 6. The nitrite+nitrate and phosphate levels showed ranges of 0.03-14.1 and 0.18-1.5 μmol kg^{-1}, respectively, and high concentrations of both were observed below 60 m at the near-glacier stations (St. 5 and St. 6). The distribution patterns of silicate were similar to the nitrite+nitrate patterns. Comparing the temperature and turbidity at subsurface layer (10 m depth), water at St. 3 and St. 4 was significantly colder and more turbid (1.2ºC and 0.82 FTU) than those at the other stations (3.0ºC and 0.22 FTU) (*U*-test, $p < 0.01$ and $p < 0.05$) (Fig. 3). Low chl *a* concentrations and high nutrient levels were found in the deeper layer (> 60 m depth), whereas in the surface layer, the chl *a* concentrations were highly variable and the nutrient concentrations were low (Fig. S1). The

relationship between chl *a* and nitrite+nitrate was significantly negative (Spearman's correlation analysis, $p < 0.05$).

3.2. Spatial distributions of protists

In this study, we identified 33 protist taxa. These included six diatom taxa (five different genera and one species), six dinoflagellate taxa (five different genera and two different species), seven oligotrich ciliate taxa (six different genera and one species), seven tintinnid ciliate taxa (five different genera and six different species), one silicoflagellate taxa, cyst/resting spore for each taxon, and nanoflagellates from different categories based on cell size and shape (Table 1). The total protist abundances and biomasses had ranged of 408−273,019 cells L^{-1} and 0.07−72.81 μgC L^{-1}, respectively. For the diatoms, their densities ranged from 0 to 526 cells L^{-1} (representing 0−14% of the total protist density), and the biomass exhibited a range of 0−14.29 μgC L^{-1} (representing 0−11% of the total protist biomass). The dinoflagellates ranged in density from 0 to 21,270 (representing 0−35% of the total protist density) and their biomass ranged from 0 to 39.30 μgC L^{-1} (representing 0−35% of the total protist biomass). The density of oligotrich ciliates ranged from 0 to 4,563 cells L^{-1} (representing 0−56% of the total protist density) and the oligotrich ciliate biomass ranged from 0 to 23.57 μgC L^{-1}

(representing 0−97% of the total protist biomass). The tintinnids ranged in density from 0 to 601 cells L^{-1} (representing 0−30% of the total protist density) and their biomass ranged from 0 to 7.15 μgC L^{-1} (representing 0−92% of the total protist biomass). For the nanoflagellates, their densities ranged from 106 to 248,505 cells L^{-1} (representing 10−98% of the total protist density), and their biomass range was 0.0007−14.04 μgC L^{-1} (representing 0.009−58% of the total protist biomass). At each station, within the total protist biomass over the whole water column, dinoflagellates and oligotrich ciliates were the dominant taxa, with mean compositions of 46.4 and 39.5%, respectively (Fig. 1). The highest total biomasses were observed near the glacier (St. 5) and at St. 1. The different taxa of the protist community exhibited varying spatial patterns. The oligotrich ciliates were abundant in the surface layer at most of the stations (Fig. 4). Large (> 60 μm equivalent spherical diameter (ESD)) dinoflagellates (*Protoperidinium* spp.) were found in the surface layer and/or at 30-70 m at all of the near-glacier stations except at St. 6 (e.g., St. 3, St. 4 and St. 5).

3.3. SEM analysis

The SEM analysis revealed a negative correlation between chl *a* and salinity (path coefficient (pc) = -0.66), i.e., the chl *a* levels increased as the salinity decreased (Fig. 5).

The diatom biomass showed positive correlations with turbidity and with the biomass of oligotrich ciliates (pc=0.48 and 0.39, respectively). Nanoflagellates had positive correlations with temperature, nitrite+nitrate, dinoflagellates and oligotrich ciliates; the correlations with temperature and dinoflagellates were particularly high (pc=0.92 and 0.76, respectively) (Fig. 5). The oligotrich ciliates showed positive correlations with diatoms (pc=0.39) and nanoflagellates (pc=0.37), whereas they were negatively correlated with temperature (pc=−0.48), salinity (pc=−0.85) and turbidity (pc=−0.37).

4. DISCUSSION

4.1. Protist biomass in the fjords around Greenland

The heterotrophic protists, which mainly comprise HNFs, ciliates and HDFs, consume a broad range of prey, ranging from bacteria to diatoms (Gast 1985, Paranjape 1987, Sherr et al. 2003; Calbet et al. 2011). Heterotrophic protists, in turn, are important prey items for mesozooplankton (Levinsen et al. 2000, Levinsen & Nielsen 2002). Thus, the heterotrophic protists play significant roles in the pelagic food webs of the Arctic Ocean (and in many other ocean systems) (Sherr et al. 1997, Rysgaard et al. 1999, Seuthe et al. 2011).

In Arctic waters, protist communities are dominated by athecate dinoflagellates

and by oligotrich ciliates, whereas thecate dinoflagellates and tintinnids show low abundances (Levinsen & Nielsen 2002). Similar patterns are observed in Disko Bay (Nielsen & Hansen 1995, Levinsen et al. 1999, Levinsen et al. 2000) and in Young Sound (Rysgaard et al. 1999) in Greenland. Despite the suboptimal preservation of oligotrich ciliates, our findings regarding protist community structures and biomass are comparable to those of previous studies.

We summarize the mean biomass of each heterotrophic species for our site and other well-studied sites around Greenland (Table 2). Our biomass values are higher than those for Young Sound (northeast Greenland) and lower than those for Disko Bay (west Greenland). Two geophysical factors influence protist biomass: glacier type (marine- vs. land-terminating) and sea-ice coverage. Inglefield Bredning is characterized by the intrusion of marine-terminating glaciers. Upwelling subglacial discharges from those glaciers affected the water properties (e.g., temperature, salinity and turbidity) and caused relatively high chl *a* concentrations at St. 4 and St. 5. Regarding sea-ice coverage, the fjord is covered by sea ice until late summer (typically July) (Sugiyama et al. 2015). Accordingly, the protist biomass in the present study was intermediate between that of the highly productive Disko Bay (short sea-ice cover duration and marine-terminating glaciers) and low-productive Young Sound (long sea-ice cover

duration and land-terminating glaciers) during summer.

4.2. Relationships between environmental parameters and the protist community

The temperature and salinity distributions revealed a cold and fresh surface water layer near glaciers. Oligotrich ciliates dominated in this layer, and the SEM analysis revealed strongly negative correlations between these ciliates and both temperature and salinity. These findings suggest that fresh surface water is a suitable habitat for oligotrich ciliates. Higher temperatures enhance the growth of ciliates in polar regions (Hansen & Jensen 2000). Matsuno et al. (2014) reported a positive relationship of ciliates with temperature in the western Arctic Ocean during autumn. Thus, the relationship between ciliates and temperature in this study was opposite to that reported in previous studies. This result means that the environmental parameters (especially temperature) are not critical factors that affect ciliates in this study region during summer.

Ciliate dominance in the region is possibly controlled by the available carbon sources. Ciliates ingest bacteria, phytoflagellates and small diatoms (Gast 1985, Paranjape 1987, Sherr et al. 2003). In this study, diatoms and nanoflagellates had positive relationships with ciliates, and the prey abundances were higher under warmer, higher-nutrient conditions, which indicates that hydrographic conditions influence prey

concentrations. Levinsen et al. (2000) suggested that the threshold concentration at which the growth rate equals zero for ciliates and HDFs is 18 µgC L^{-1}. Assuming that all of the oligotrich ciliates, tintinnids and dinoflagellates in this study were heterotrophic organisms, the average contribution of the ciliates to the carbon biomass of the heterotrophic organisms in this study was 53.5%. The threshold concentration for ciliates is estimated to be 9.63 µgC L^{-1} (=18*0.535). In this study, the maximum biomass of potential prey (i.e., diatoms and nanoflagellates) for ciliates was 14.07 µgC L^{-1} at 0 m at St.1, and the average biomass throughout the study region was 0.936 µgC L^{-1}. Since the average prey concentration was much lower than the threshold concentration needed for ciliate growth, ciliate growth would have been limited by the low prey concentrations (Levinsen et al. 2000).

We did not examine the bacterial abundances in this study. Bacterial production is reported to be high (0.13 µgC L^{-1} day^{-1}) in the surface layer of Young Sound (northeastern Greenland) during summer despite low dissolved organic carbon (DOC) concentrations from river inflows (Paulsen et al. 2017). High bacterial productivity may contribute to the dominance of ciliates in the surface layer, supporting HNF linkage between bacteria and ciliates (Nielsen & Hansen 1995). Seasonally, the maximum ciliate biomasses were seen in surface water after diatom blooms and under decreased

grazing pressure from copepods following the migration of large copepods (*Calanus* spp.) to the deeper layers (Levinsen et al. 1999). Despite no information on the grazing pressure by copepods in this study, the ciliate abundances are believed to be controlled by bottom-up effects, not only by sufficient food concentrations (diatoms and nanoflagellates) but also by HNF thriving via high bacterial production.

4.3. Effects of glacial meltwater discharge on protists

Heterotrophic dinoflagellates dominate the microzooplankton biomass in the Arctic Ocean during summer (Andersen 1988, Nielsen & Hansen 1995, Sherr et al. 1997). Levinsen et al. (1999) reported that HDFs represented on average 70% of the integrated microzooplankton biomass when the diatoms formed subsurface blooms. After the diatoms declined, the large HDFs became less abundant. In the present study, the diatom abundances were low throughout the study region, suggesting that the HDF abundances were likely low due to food limitations (Levinsen et al. 1999). The SEM analysis revealed that the dinoflagellates had a significant positive relationship with the nanoflagellates but not with diatoms. This result suggests that the HDF population was maintained by grazing nanoflagellates after the diatom blooms (Levinsen & Nielsen 2002). According to Jakobsen and Hansen (1997), the ability of HDFs to cope with

starvation is greater than that of planktonic ciliates because under starvation conditions, dinoflagellates can extend their minimum generation time to beyond that of the ciliates. Thus, HDFs can survive due to their flexible grazing strategy (changing prey types in response to availability) and their strong tolerance to starvation in fjords during the summer.

Freshwater discharges from the bottom of marine-terminating glaciers induce strong upwelling near the glacier fronts, which transports nutrient-rich deep-layer water into the euphotic layer (Bendtsen et al. 2015, Meire et al. 2017; Kanna et al., 2018). In this study, upwelling water was represented by a highly turbid and low-temperature subsurface layer observed near glaciers. Due to the nutrient input into the euphotic layer, the chl *a* concentrations and primary production increased within the relatively thin subsurface layer (Calbet et al. 2011, Meire et al. 2017). As with previous studies, the chl *a* concentrations in the subsurface layer (10 m) were slightly higher at the near-glacier stations (i.e., St. 4 and St. 5) than at the other stations (0.99 vs 0.67, *U*-test, $p = 0.39$). The nutrient concentrations were uniformly distributed among the stations, but relatively high concentrations were found at St. 4 and St. 5 (0.85 vs 0.14, *U*-test, $p = 0.13$). These observations suggest that the relatively high chl *a* levels were maintained by nutrients upwelling near the glacier. Previous studies have indicated that the euphotic

depth is very important for chl *a* distribution. During summer in Disko Bay, the euphotic zone is situated at around 30 m (Levinsen et al. 1999). Although we did not measure vertical profiles of light intensity in the water column, high chl *a* concentrations were found in the highly turbid layer. This observation suggests that high turbidity did not prevent primary production by phytoplankton, at least in the subsurface layer. We did not measure primary production and do not have field data from other seasons. Nevertheless, our study results suggest that the nutrient concentrations in the upwelling water near the glacier play a critical role in primary production in Inglefield Bredning during summer.

Nanoflagellates are important components of the food web in fjords because they are grazed upon by larger heterotrophic species, as mentioned above. They are abundant in the summer fjords, particularly where plumes occur in front of glaciers (e.g., Middelbo et al. 2018). In Young Sound, phytoplankton smaller than 10 µm were dominant near the glacier throughout the year (Middelbo et al. 2018, 2019, Holding et al. 2019). Near the glacier, strong stratification due to fresh surface water prevents upwelling of nutrients to the surface layer. Thus, small phytoplankton dominate in a low-nutrient surface layer (Daufresne et al. 2009; Li et al. 2009; Gardner et al. 2011). Compared to micro-sized autotrophs (e.g., diatoms), the small cells of nanoflagellates (<

10 μm) and even smaller picophytoplankton (< 2 μm) are adapted to low-light intensities and are capable of generating efficient primary production (Taguchi 1976, Raven 1998, Holding et al. 2019). The SEM analysis revealed that the nanoflagellates had positive relationships with temperature and nitrite+nitrate. Since the trophic type of the nanoflagellates were unidentifiable in this study, two feasible reasons could explain regarding to heterotrophic and autotrophic nanoflagellates, respectively. Firstly, high-temperature conditions potentially increase the growth rate of HNFs (Choi & Peters 1992). Because of that, the strong relationship between temperature and nanoflagellates in the SEM means that the HNFs potentially increase in the high temperatures. From the different aspect of the nanoflagellates, secondary, the nitrite+nitrate levels potentially stimulated the primary production by autotrophic nanoflagellates (Middelbo et al 2018, 2019, Holding et al. 2019).

On the other hand, large-sized *Protoperidium* spp. were found only at stations near glaciers where nutrients were supplied by upwelling water. Large *Protoperidium* spp. (mean 104 μm ESD) can graze on small dinoflagellates (e.g., *Gymnodinium* spp., mean 31 μm ESD) and on small ciliates (e.g., *Strombidium* spp., mean 41 μm ESD) (Levinsen & Nielsen 2002); the small dinoflagellates and ciliates graze on nanoflagellates (Jakobsen & Hansen 1997). Based on these facts, we speculate that the

nanoflagellates (we assume autotrophic and mixotrophic nanoflagellates here) used the upwelling nitrite+nitrate and that the resulting production was transported to the large *Protoperidium* spp. via the small dinoflagellates and ciliates. While as the heterotrophic nanoflagellates, the HNFs have a strong link to bacteria and to the small dinoflagellates and ciliates (Nielsen & Hansen 1995); bacterial production was supported by the labile carbon supplied by meltwater from glaciers (Paulsen et al. 2017, 2019). Therefore, both autotrophic and heterotrophic nanoflagellates could be increased by the upwelling nutrients and the high bacterial production, resulting in the abundance of large HDFs only near glaciers. We conclude that the upwelling subglacial discharge not only affects the chl *a* concentrations but can also stimulate nanoflagellate production, ultimately increasing production via HDFs and ciliates.

Acknowledgements

We thank Toku Oshima, Kim Peterson, Sakiko Daorana, Takuto Ando, Yoshiki Fujisi and Izumi Asaji, who assisted with the field observations. This study was financially supported by the Arctic Challenge for Sustainability (ArCS) project led by Drs. Kumiko Azuma and Toru Hirawake. Part of this study was supported by a Grant-in-Aid for Scientific Research grants 19H03037 (B), 18K14506 (Early Career Scientists), and

17H01483 (A) from the Japanese Society for the Promotion of Science (JSPS). Part of this study was supported by the KOPRI Asian Polar Science Fellowship Program 2019.

References

Andersen P (1988) The quantitative importance of the ‘‘microbial loop’’ in the marine pelagic: a case study from the north Bering/Chukchi Seas. Arch Hydrobiol 31:243−251

Arendt KE, Nielsen TG, Rysgaard S, Tönnesson K (2010) Differences in plankton community structure along the Godthåbsfjord, from the Greenland Ice Sheet to offshore waters. Mar Ecol Prog Ser 401:49−62

Arendt KE, Juul-Pedersen T, Mortensen J, Blicher ME, Rysgaard S (2013) A 5-year study of seasonal patterns in mesozooplankton community structure in a sub-Arctic fjord reveals dominance of *Microsetella norvegica* (Crustacea, Copepoda). J Plankton Res 35:105−120

Arendt KE, Agersted MD, Sejr MK, Juul-Pedersen T (2016) Glacial meltwater influences on plankton community structure and the importance of top-down control (of primary production) in a NE Greenland fjord. Estuar Coast Shelf Sci 183:123−135

Bendtsen J, Mortensen J, Lennert K, Rysgaard S (2015) Heat sources for glacial ice melt in a West Greenland tidewater outlet glacier fjord: The role of subglacial freshwater discharge. Geophys Res Lett 42:4089−4095

Calbet A, Riisgaard K, Saiz E, Zamora S, Stedmon C, Nielsen TG (2011) Phytoplankton growth and microzooplankton grazing along a sub-Arctic fjord (Godthåbsfjord, west Greenland). Mar Ecol Prog Ser 442:11−22

Choi JW, Peters F (1992) Effects of temperature on two psychrophilic ecotypes of a heterotrophic nanoflagellate, *Paraphysomonas imperforate*. Appl Environ Microbiol 58:593−599

Cowton TR, Sole AJ, Nienow PW, Slater DA, Christoffersen P (2018) Linear response of east Greenland's tidewater glaciers to ocean/atmosphere warming. Proc Natl Acad Sci 115:7907−7912

Daufresne M, Lengfellner K, Sommer U (2009) Global warming benefits the small in aquatic ecosystems. Proc Natl Acad Sci USA 106:12788−12793

Evagelopoulos A (2002) Taxonomic notes on *Protoperidinium* (Peridiniales, Dinophyceae) species in the Thermaikos Bay (North Aegean Sea, Greece). Mediterr Mar Sci 3:41−54

Fukuyo Y, Inoue H, Takayama H (1997) Class Dinophyceae. In: Chihara M, Murano M (eds) An illustrated guide to marine plankton in Japan. Tokai University Press, Tokyo, p 31–112

Gardner JL, Peters A, Kearney MR, Joseph L, Heinsohn R (2011) Declining body size:

a third universal response to warming? Trends Ecol Evol 26:285–291

Gast V (1985) Bacteria as a food source for microzooplankton in the Schlei Fjord and Baltic Sea with special reference to ciliates. Mar Ecol Prog Ser 22:107−120

Hansen BW, Jensen F (2000) Specific growth rates of protozooplankton in the marginal ice zone of the central Barents Sea during spring. J Mar Biol Assoc UK 80:37−44

Hasle GR, Syvertsen EE (1997) Marine diatoms. In: Tomas CR (ed) Identifying marine phytoplankton. Academic Press, San Diego, p 5−385

Holding JM, Markager S, Pedersen TJ-, Paulsen ML, Møller EF, Meire L, Sejr MK (2019) Seasonal and spatial patterns of primary production in a high-latitude fjord affected by Greenland Ice Sheet run-off. Biogeosciences 16:3777–3792

Howat IM, Eddy A (2011) Multi-decadal retreat of Greenland's marine-terminating glaciers. J Glaciol 57:389−396

Jakobsen HH, Hansen PJ (1997) Prey size selection, grazing and growth response of the small heterotrophic dinoflagellate *Gymnodinium* sp. and the ciliate *Balanion comatum* − a comparative study. Mar Ecol Prog Ser 158:75−86

Juul-Pedersen T, Arendt KE, Mortensen J, Blicher ME, Søgaard DH, Rysgaard S (2015) Seasonal and interannual phytoplankton production in a sub-Arctic tidewater

outlet glacier fjord, SW Greenland. Mar Ecol Prog Ser 524:27−38

Kanna N, Sugiyama S, Ohashi Y, Sakakibara D, Fukamachi Y, Nomura D (2018) Upwelling of macronutrients and dissolved inorganic carbon by a subglacial freshwater driven plume in Bowdoin Fjord, northwestern Greenland. J Geophys Res 123:1666−1682

Krawczyk DW, Arendt KE, Juul-Pedersen T, Sejr MK, Blicher ME, Jakobsen HH (2015) Spatial and temporal distribution of planktonic protists in the East Greenland fjord and offshore waters. Mar Ecol Prog Ser 538:99−116

Levinsen H, Nielsen TG (2002) The trophic role of marine pelagic ciliates and heterotrophic dinoflagellates in arctic and temperate coastal ecosystems: A cross-latitude comparison. Limnol Oceanogr 47:427−439

Levinsen H, Nielsen TG, Hansen BW (1999) Plankton community structure and carbon cycling on the western coast of Greenland during the stratified summer situation. II. Heterotrophic dinoflagellates and ciliates. *Aquat Microb Ecol* 16:217−232

Levinsen H, Nielsen TG, Hansen BW (2000) Annual succession of marine pelagic protozoans in Disko Bay, West Greenland, with emphasis on winter dynamics. Mar Ecol Prog Ser 206:119−134

Li WKW, McLaughlin FA, Lovejoy C, Carmack EC (2009) Smallest algae thrive as the Arctic ocean freshens. Science 326:539−539

Lydersen C, Assmy P, Falk-Petersen S, Kohler J, Kovacs KM, Reigstad M, Steen H, Strøm H, Sundfjord A, Varpe Ø, Walczowski W, Weslawski JM, Zajaczkowski M (2014) The importance of tidewater glaciers for marine mammals and seabirds in Svalbard, Norway. J Mar Syst 129:452−471

Maeda M (1997) Suborder Oligotrichida. In: Chihara M, Murano M (eds) An illustrated guide to marine plankton in Japan. Tokai University Press, Tokyo, p 397−420

Matsuno K, Ichinomiya M, Yamaguchi A, Imai I, Kikuchi T (2014) Horizontal distribution of microprotist community structure in the western Arctic Ocean during late summer and early fall of 2010. Polar Biol 37:1185−1195

Matsuno K, Abe Y, Yamaguchi A, Kikuchi T (2016) Regional patterns and controlling factors on summer population structure of *Calanus glacialis* in the western Arctic Ocean. Polar Sci 10:503−510

Meire L, Mortensen J, Meire P, Juul-Pedersen T, Sejr MK, Rysgaard S, Nygaard R, Huybrechts R, Meysman FJ (2017) Marine-terminating glaciers sustain high productivity in Greenland fjords. Glob Change Biol 23:5344−5357

Menden-Deuer S, Lassard EJ (2000) Carbon to volume relationships for dinoflagellates,

diatoms, and other protest plankton. Limnol Oceanogr 45:569−579

Middelbo AB, Sejr MK, Arendt KE, Møller EF (2018) Impact of glacial meltwater on spatiotemporal distribution of copepods and their grazing impact in Young Sound NE, Greenland. Limnol Oceanogr 63:322−336

Middelbo AB, Møller EF, Arendt KE, Thyrring J, Sejr MK (2019) Spatial, seasonal and inter-annual variation in abundance and carbon turnover of small copepods in Young Sound, Northeast Greenland. Polar Biol 42:179–193

Mortensen J, Lennert K, Bendtsen J, Rysgaard S (2011) Heat sources for glacial melt in a sub-Arctic fjord (Godthåbsfjord) in contact with the Greenland Ice Sheet. J Geophys Res 116, C01013, doi:10.1029/2010JC006528

Naito A, Abe Y, Matsuno K, Nishizawa B, Kanna N, Sugiyama S, Yamaguchi A (2019) Surface zooplankton size and taxonomic composition in Bowdoin Fjord, north-western Greenland: A comparison of ZooScan, OPC and microscopic analyses. Polar Sci 19:120−129

Nielsen TG, Hansen BW (1995) Plankton community structure and carbon cycling on the western coast of Greenland during and after the sedimentation of a diatom bloom. Mar Ecol Prog Ser 125:239−257

Nielsen TG, Ottosen LD, Hansen BW (2007) Structure and function of the pelagic

ecosystem in Young Sound, NE Greenland. Meddr Grønland Bioscience 58:88−107

Olson MB, Strom SL (2002) Phytoplankton growth, microzooplankton herbivory and community structure in the southeast Bering Sea: insight into the formation and temporal persistence of an *Emiliania huxleyi* bloom. Deep Sea Res II 49:5969−5990

Paranjape MA (1987) Grazing by microzooplankton in the eastern Canadian arctic in summer 1983. Mar Ecol Prog Ser 40:239−246

Paulsen ML, Nielsen SEB, Müller O, Møller EF, Stedmon CA, Juul-Pedersen T, Markager S, Sejr MK, Delgado-Huertas A, Larsen A, Middelboe M (2017) Carbon bioavailability in a high Arctic fjord influenced by glacial meltwater, NE Greenland. Front Mar Sci 4, 176, doi: 10.3389/fmars.2017.00176

Paulsen ML, Müller O, Larsen A, Møller EF, Middelboe M, Sejr MK, Stedmon C (2019) Biological transformation of Arctic dissolved organic matter in a NE Greenland fjord. Limnol Oceanogr 64:1014−1033

Pedersen SA, Ribergaard MH, Simonsen CS (2005) Micro- and mesozooplankton in Southwest Greenland waters in relation to environmental factors. J Mar Syst 56:85−112

Pomeroy LR (1974) The ocean's food web: a changing paradigm. Bioscience 24:499−503

Raven JA (1998) Small is beautiful: the picophytoplankton, Funct Ecol 12:503−513

Rysgaard S, Nielsen TG, Hansen BW (1999) Seasonal variation in nutrients, pelagic primary production and grazing in a high-Arctic coastal marine ecosystem, Young Sound, Northeast Greenland. Mar Ecol Prog Ser 179:13−25

Rysgaard S, Nielsen TG (2006) Carbon cycling in a high-arctic marine ecosystem−Young Sound, NE Greenland. Prog Oceanogr 71:426−445

Sakakibara D, Sugiyama S (2018) Ice front and flow speed variations of marine-terminating outlet glaciers along the coast of Prudhoe Land, northwestern Greenland. J Glaciol 64:300−310

Seuthe L, Iversen K R, Narcy F (2011) Microbial processes in a high-latitude fjord (Kongsfjorden, Svalbard): II. Ciliates and dinoflagellates. Polar Biol 34:751−766

Sherr EB, Sherr BF, Fessenden L (1997) Heterotrophic protist in the central Arctic Ocean. Deep Sea Res II 44:1665−1682

Sherr EB, Sherr BF, Wheeler PA, Thompson K (2003) Temporal and spatial variation in stocks of autotrophic and heterotrophic microbes in the upper water column

of the central Arctic Ocean. Deep Sea Res I 50:557−571

Stoecker DK, Gifford DJ, Putt M (1994) Preservation of marine planktonic ciliates: losses and cell shrinkage during fixation. Mar Ecol Prog Ser 110:293−299

Stomp M, Huisman J, Mittelbach GG, Litchman E, Klausmeier CA, (2011) Largescale biodiversity patterns in freshwater phytoplankton. Ecology 92:2096−2107

Sugiyama S, Sakakibara D, Tsutaki S, Maruyama M, Sawagaki T (2015) Glacier dynamics near the calving front of Bowdoin Glacier, northwestern Greenland. J Glaciol 61:223−232

Sun J, Liu D (2003) Geometric models for calculating cell biovolume and surface area for phytoplankton. J Plankton Res 25:1331−1346

Taguchi S (1976) Relationship between photosynthesis and cell size of marine diatoms, J Phycol 12:185−189

Taniguchi A (1984) Microzooplankton biomass in the Arctic and subarctic Pacific Ocean in summer. Mem Natl Inst Polar Res (special issue) 32:63−80

Taniguchi A (1997) Suborder Tintinnina. In: Chihara M, Murano M (eds) An illustrated guide to marine plankton in Japan. Tokai University Press, Tokyo, p 421−483

Welshmeyer NA (1994) Fluorometric analysis of chlorophyll *a* in the presence chlorophyll *b* and phaeopigments. Limnol Oceanogr 39:1985–1992

Table 1. Species of protists observed in Inglefield Bredning, northwestern Greenland, during 13-17 August 2018.

Diatoms	Tintinnids
Cocconeis spp.	*Codonella galea*
Cylindrotheca closterium	*Favera azorica*
Navicula spp.	*Parafavera denticulata*
Odontella spp.	*Parafavera hadai*
Pennate diatoms	*Parafavera jorgenseni*
Thalasiosira spp.	*Ptychocylis obtusa*
Dinoflagellates	*Tintinnopsis* spp.
Amphidinium spp.	Silicoflagellates
Dinophysis spp.	*Dictyoca* spp.
Gymnodinium spp.	Other
Gyrodinium spp.	Ciliate cysts
Protoperidinium depressum	Diatom resting spores
Protoperidinium divergens	Dinoflagellates cysts
Ciliates	Nanoflagellates (slender, 5-10 µm)
Laboera strobila	Nanoflagellates (spherical, < 5 µm)
Leegardiera spp.	Nanoflagellates (spherical, 5-10 µm)
Lohmanniella spp.	
Mesodinium spp.	
Scuticociliates	
Strobilidium spp.	
Strombidium spp.	

1 Table 2. A summary of the biomass standing stock of ciliates, dinoflagellates and
2 nanoflagellates (NF) around Greenland. MTG: marine-terminating glacier, LTG:
3 land-terminating glacier. Mean biomass shown integrated biomass for each taxon.

Area	Glacier type	Depth	Period	Integrated biomass (mgC m^{-2})			Reference
				Ciliates	Dinoflagellates	NF	
W Greenland (Disko Bay)	MTG	0-30 m	July	330	393	246[a]	Nielsen & Hansen 1995
		0-28 m	August	270	500		Levinsen & Nielsen 2002
		0-30 m	July-September	286	486		Levinsen et al. 1999
		0-200 m	August	620	910		Levinsen et al. 2000
SW Greenland	MTG	0-200 m	June	243	386	134[b]	Pedersen et al. 2005
NE Greenland (Young Sound)	LTG	0-35 m	June	98	40	48[b]	Nielsen et al. 2007
		0-35 m	August	20-143	20-70		Rysgaard et al. 1999
NW Greenland (Inglefield Bredning)	MTG	0-100 m	August	241	294	74[c]	This study

4 a: autotrophic/mixotrophic, b: heterotrophic, c: autotrophic/mixotrophic/heterotrophic

5

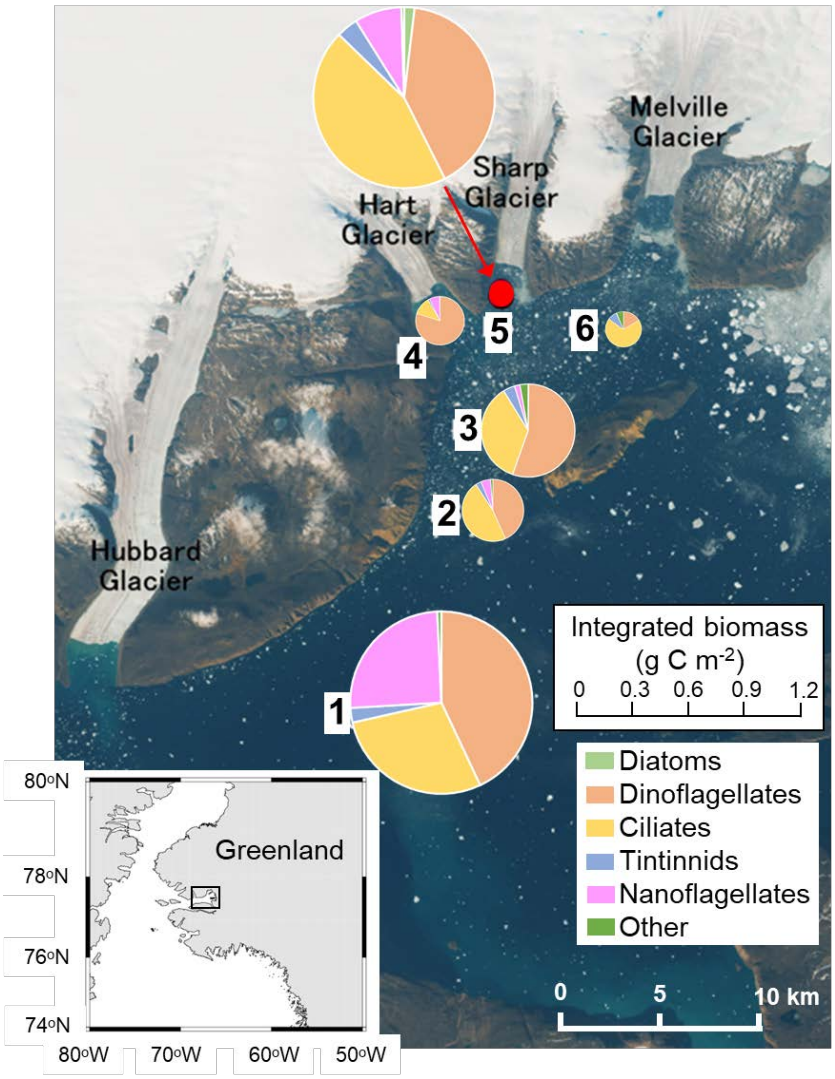

Fig. 1. Horizontal distributions of the integrated carbon biomass and species compositions of the protist community in the water column (0-100 m for all stations except St. 4 (0-40 m)) in Inglefield Bredning, northwestern Greenland, obtained during 13-17 August 2018. The numbers indicate the station names. The background image is from Modified Copernicus Sentinel data (13 August 2018), processed with Sentinel flow (https://github.com/juseg/sentinelflow). The inset shows the location of the study site.

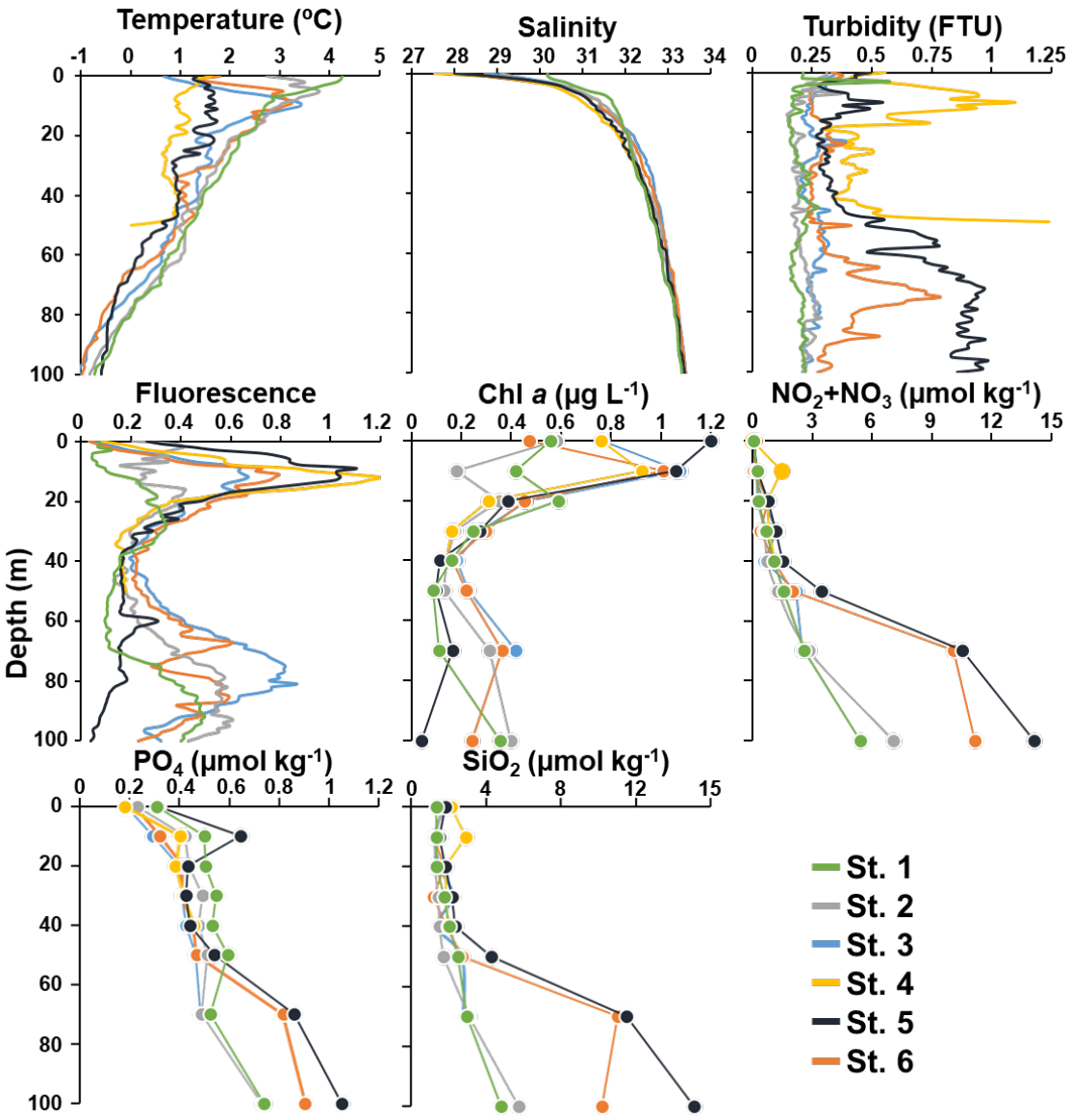

Fig. 2. Vertical profiles of environmental parameters in Inglefield Bredning, northwestern Greenland, obtained during 13-17 August 2018. The dots in the plots of chlorophyll *a* and nutrients are data obtained from water samples.

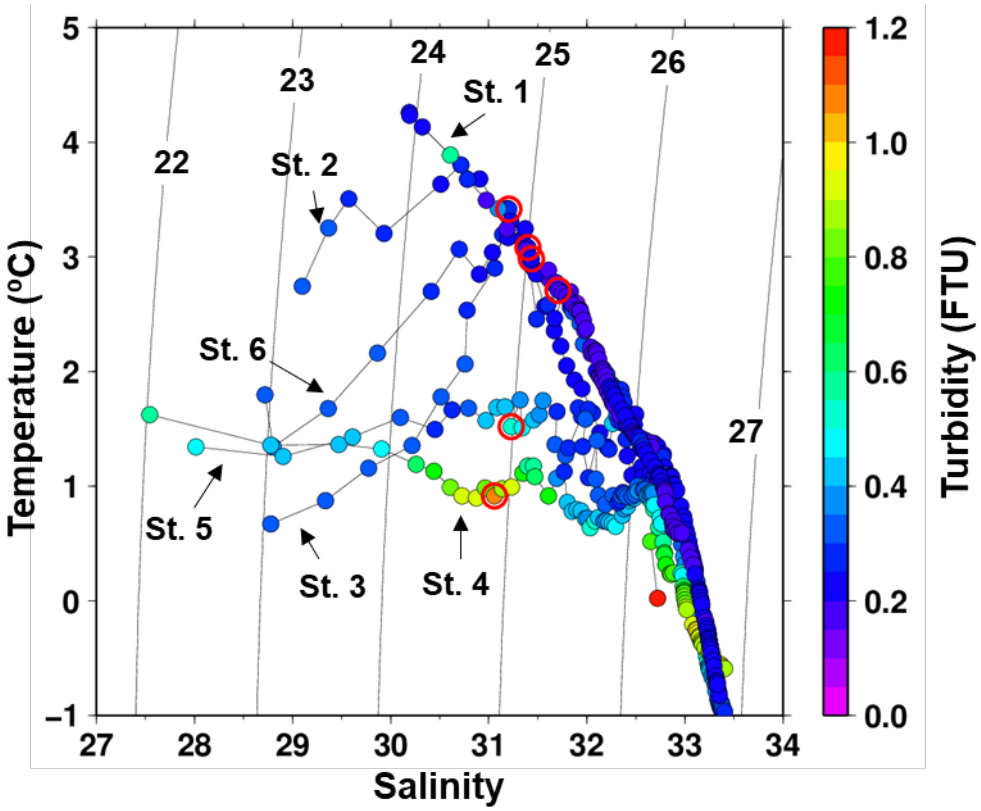

Fig. 3. T-S diagram with turbidity in Inglefield Bredning, northwestern Greenland, during 13-17 August 2018. Red circles indicate the value at 10 m depth.

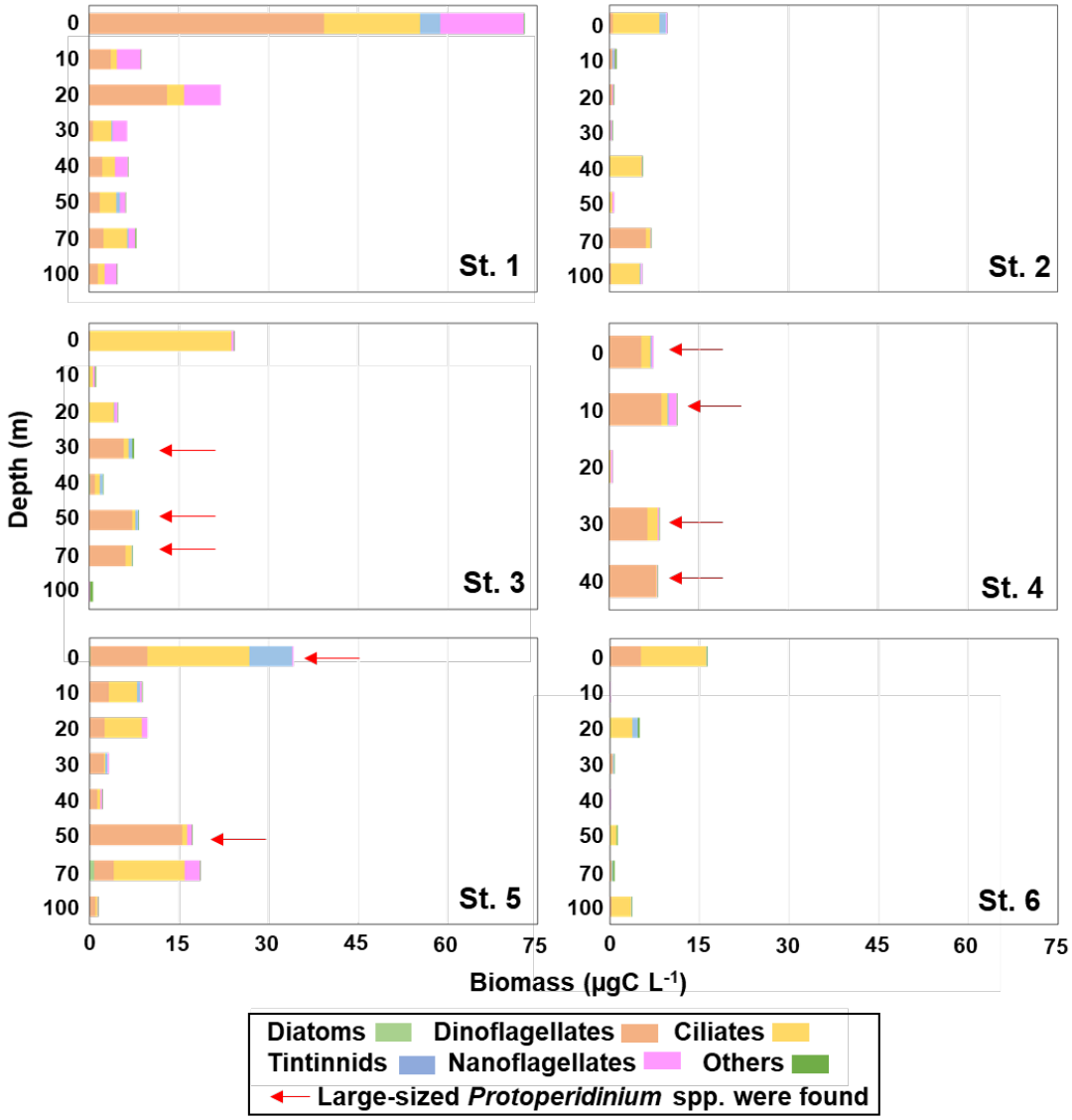

Fig. 4. Vertical distributions of the protist community in Inglefield Bredning, northwestern Greenland, during 13-17 August 2018. The red arrows indicate the large-sized *Protoperidinium* spp were found.

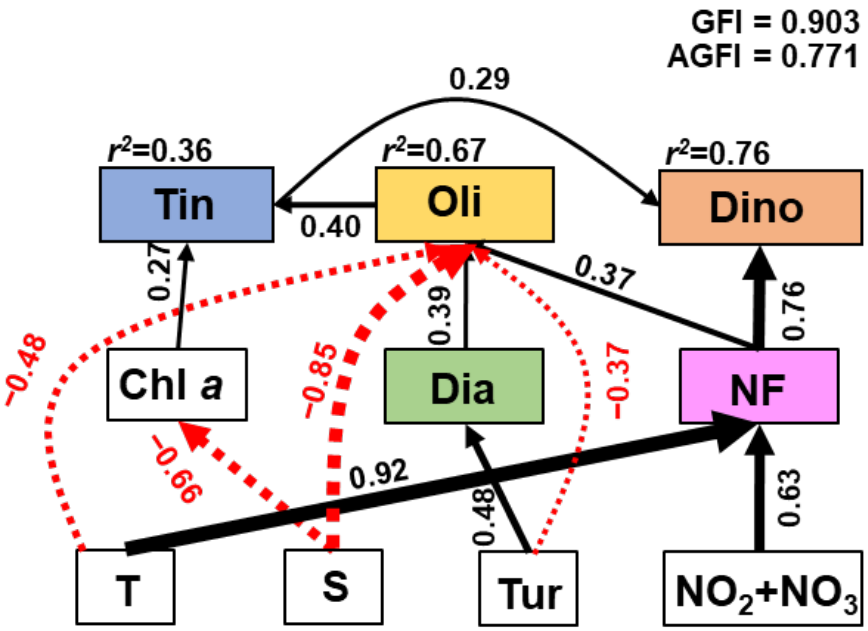

Fig. 5. Results of the structural equation modeling (SEM) of protist biomasses and environmental factors. The numbers along the pathways represent the standardized path coefficients. The arrows with solid and dashed lines indicate positive and negative effects, respectively. The arrow thicknesses vary with the path coefficient values. The overall fit of the model was evaluated using the goodness-of-fit index (GFI) and the adjunct goodness-of-fit index (AGFI). T: temperature, S: salinity, Tur: turbidity, NO_2+NO_3: nitrite and nitrate, Chl *a*: chlorophyll *a*, Dia: diatoms, NF: nanoflagellates, Dino: dinoflagellates, Oli: oligotrich ciliates, and Tin: tintinnids.